Synthesis of a Stable Form of Tertiapin: A High-Affinity Inhibitor for Inward-Rectifier K^+ Channels[†]

Weili Jin and Zhe Lu*

Department of Physiology, University of Pennsylvania, 3700 Hamilton Walk, Philadelphia, Pennsylvania 19104

Received May 25, 1999; Revised Manuscript Received July 22, 1999

ABSTRACT: Tertiapin (TPN), a small protein derived from honey bee venom, inhibits the GIRK1/4 and ROMK1 channels with nanomolar affinities. Methionine residue 13 in TPN interacts with residue F148 in the channel, located just outside of the narrow region of the ROMK1 pore. The methionine residue in TPN can be oxidized by air, which significantly hinders TPN binding to the channels. To overcome the reduction in TPN affinity due to oxidation of M13, we replaced M13 in TPN with fourteen different residues. Out of the fourteen derivatives, only the one in which M13 was replaced by glutamine, TPN_Q, binds to the channel with a K_i value very similar to that of native TPN. Since TPN_Q is stable and functionally resembles native TPN, it will be a very useful molecular probe for studying the inward-rectifier K^+ channels.

Inward-rectifiers are a class of K^+ channels that differ structurally as well as functionally from the voltage-activated K^+ channels (*1*−*7*). The primary sequences of the subunit in the two classes of channels are minimally conserved, except for the *signature sequence* within the P-region that forms the "K^+-selectivity filter" (*8*, *9*). Furthermore, each of the four subunits in the inward-rectifier K^+ channels has only two (M1 and M2) instead of the six (S1 through S6) transmembrane segments occurring in the voltage-activated K^+ channels (*2*−*7*). A recent crystallographic study on a bacterial K^+ channel (KcsA) showed that the outer and narrow part of the K^+ pore is formed by the signature sequence, whereas the inner part of the pore is formed by the M2 segment (*9*).

Unlike the voltage-activated K^+ channels, which are primarily responsible for repolarizing the action potential, the inward-rectifier K^+ channels maintain and regulate the resting membrane potential (*1*). By doing so, the inward-rectifier K^+ channels play many important biological roles. For example, the G-protein-gated inward-rectifier K^+ channels mediate vagal inhibition of the cardiac pacemaker and modulate synaptic transmission in the nervous system, whereas the ROMK1 inward-rectifier channels are critical for the kidneys to maintain water and electrolyte balance (*1*, *2*).

Thus far, about twenty different kinds of protein inhibitors (or toxins) for the voltage-activated K^+ channels have been isolated from the venoms of various poisonous animals (e.g., 10−37). These protein inhibitors prove to be very effective probes for understanding both the physiology as well as the structure−function relationship of voltage-activated K^+ channels (*38*−*54*). In contrast, the pharmacology of inward-rectifier K^+ channels is poorly developed (*55*, *56*). Recently, we found that tertiapin (TPN), a small protein derived from honey bee venom, inhibits the G-protein-gated inward-rectifier K^+ channel (GIRK1/4) and the ROMK1 channel with nanomolar affinities (*57*; cf. *58* and *59* for its original discovery). However, a methionine residue in TPN can be readily oxidized by air. Oxidation of TPN significantly hinders its binding to the channels. To overcome this problem, we synthesized a high affinity TPN derivative in which the air-oxidizable methionine residue is replaced by a glutamine residue.

MATERIALS AND METHODS

Channel Expression. Oocytes harvested from *Xenopus laevis* frogs were digested with collagenase (2 mg/mL) in a solution containing 82.5 mM NaCl, 2.5 mM KCl, 1.0 mM $MgCl_2$, and 5.0 mM (pH 7.6) HEPES. The oocyte digestion solution was agitated on a platform shaker at a rate of 80 rpm for 90 min. The oocytes were then rinsed thoroughly with and stored in a solution containing 50 μg/mL gentamicin, 96 mM NaCl, 2 mM KCl, 1.8 mM $CaCl_2$, 1 mM $MgCl_2$, and 5 mM (pH 7.6) HEPES. Defolliculated oocytes were selected at least 2 h after the collagenase digestion. To express the channels, the corresponding cRNA was directly injected into oocytes. To express the GIRK1/4 channel, GIRK1 and GIRK4 cRNAs were coinjected with either M2 or M4 muscarinic receptor cRNA. All injections were carried out at least 16 h after the collagenase treatment. The injected oocytes were stored in an 18 °C incubator.

Channel Recording. All three inward-rectifier K^+ channels, GIRK1/4, ROMK1, and IRK1, were studied using a two-electrode voltage clamp amplifier (Oocyte Clamp OC-725C, Warner Instruments Corp.) The resistance of electrodes, filled with 3 M KCl, was 0.3−0.5 MΩ. To elicit current through the channel, the membrane potential of oocytes was stepped

[†] This study was supported by an NSF grant (IBN-97-27436) and an NIH grant (GM55560). Z. Lu was a recipient of an Independent Scientist Award from NIH (HL03814).

* Please send correspondence to: Dr. Zhe Lu, University of Pennsylvania, Department of Physiology, D302A Richards Building, 3700 Hamilton Walk, Philadelphia, PA 19104. Telephone: 215-573-7711. Fax: 215-573-5851. E-mail: zhelu@mail.med.upenn.edu.

10.1021/bi991205r CCC: $18.00
Published on Web 10/08/1999

to −80 mV and then to +80 mV from the holding potential of 0 mV. Background leak currents were obtained by exposing oocytes to solutions containing TPN or TPN_Q at concentrations greater than 100-fold of K_i. The bath solution contained 100 mM KCl, 0.3 mM $CaCl_2$, 1.0 mM $MgCl_2$, and 10 mM (pH7.6) HEPES. To activate the GIRK1/4 channel, ACh (150 μM) was included in the bath solution. The concentration of TPN and its derivative was calculated by converting the absorbance of the solution at 280 nm wavelength using an extinction coefficient 6.1 mM^{-1} cm^{-1}. In the case where methionine 13 was replaced by aromatic residues, the concentration of the derivatives was estimated by normalizing the peak area of a sample (in a predetermined volume) detected at 215 nm wavelength on HPLC to that of a known quantity of TPN sample. All toxin-containing solutions were freshly made by diluting stock solutions. TPN and its derivatives used in all experiments were made synthetically (see below).

Molecular Biology. The GIRK1 and GIRK4 (CIR) cDNAs were cloned into pBluescript (SK-) plasmid (Stratagene)(*4*, *6*). The ROMK1 and IRK1 cDNAs were cloned into pSPORT (Gibco-BRL) and pcDNA1/AMP (Invitrogen) plasmids, respectively (*2*, *3*). The M2 and M4 receptor cDNAs were cloned into a pGEM3 (Promega) plasmid. The GIRK1, ROMK1, and IRK1 cDNAs were linearized using *Not*I. The GIRK4 cDNA was linearized using *Xho*I. The M2 and M4 receptor cDNAs were linearized using *Hind*III. All cRNAs, except for that of GIRK4, were synthesized using T7 polymerase (Promega). The GIRK4 cRNA was synthesized using T3 polymerase (Promega).

Synthesis, Mass Determination, and Purification of Tertiapin and Tertiapin Derivatives. Tertiapin and its derivatives were synthesized using a Rainin/Protein Technologies Symphony multipeptide synthesizer, and their mass was confirmed on a VG analytical MALDI-TOF spectrometer. Synthetic TPN and its derivatives have a C-terminal amide group. All synthetic peptides spontaneously adopted the correct conformation in a solution containing 1 mM DTT and 10 mM Tris (pH 8.0) after DTT became oxidized. After the peptides folded into the correct conformation, they were purified with a reverse phase HPLC column (C18) using a linear methanol gradient (1% per minute). The flow rate was 1 mL/min. The nonoxidized TPN used in the experiment was assayed daily on HPLC. The sample is considered nonoxidized only if the oxidized form is less than 1%. The oxidized TPN used in the experiment was spontaneously air-oxidized and purified by HPLC.

RESULTS

Spontaneous Oxidation of the Methionine Residue in Tertiapin. Figure 1A shows an HPLC chromatograph of TPN. With time, TPN is "spontaneously" converted into an earlier peak observed on HPLC. The chromatograph of TPN samples either partially or fully converted are shown in Figure 1, B and C, respectively. Mass analysis of the material corresponding to the new peak shows its mass is 16 daltons (the mass of an oxygen atom) greater than the expected for TPN, while the material corresponding to the original peak has the mass of TPN. This finding argues that the new peak results from oxidation of TPN. Since the four cysteine residues forming two disulfide bonds are already in an oxidized form, methionine 13 is likely to be the residue

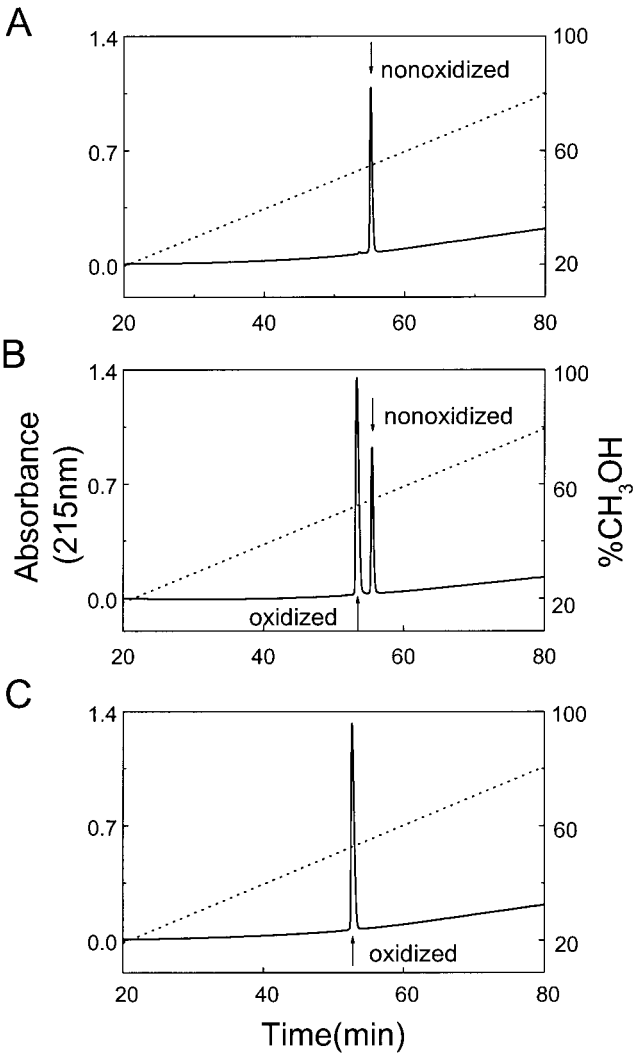

FIGURE 1: Chromatography of oxidized and nonoxidized TPN. Samples were nonoxidized (A), partially oxidized (B), and oxidized (C) TPN. Mobile phases A and B were 0.1% TFA in water and 0.07% TFA in methanol. The samples were eluted by increasing mobile phase B at a rate of 1% per minute.

oxidized by air. To test this possibility, we substituted M13 with fourteen other residues (A, D, E, F, G, I, L, N, Q, S, T, V, W, and Y). Each of these TPN derivatives has an invariable retention time on HPLC, strongly supporting the idea that the oxidization occurs in the side-chain of M13.

Oxidation of M13 hinders the binding of TPN to the channels. Figure 2, A and B shows the current traces of the GIRK1/4 and ROMK1 channels in the absence and presence of nonoxidized TPN. Comparatively, Figure 2, C and D shows the current traces in the absence and presence of oxidized TPN. To achieve a similar extent of channel blockade higher concentrations of oxidized TPN must be applied. The fractions of the unblocked current of the GIRK1/4 channel are plotted against the concentrations of the oxidized and nonoxidized TPN in Figure 2E, while those of the ROMK1 channel are plotted in Figure 2F. The curves superimposed on the data points in Figure 2, E and F correspond to the fits of an equation assuming that one TPN molecule blocks one channel.

Identification of the Channel Residue Energetically Coupled to Residue 13 in TPN. To identify the channel residue energetically coupled to residue 13 in TPN, we used

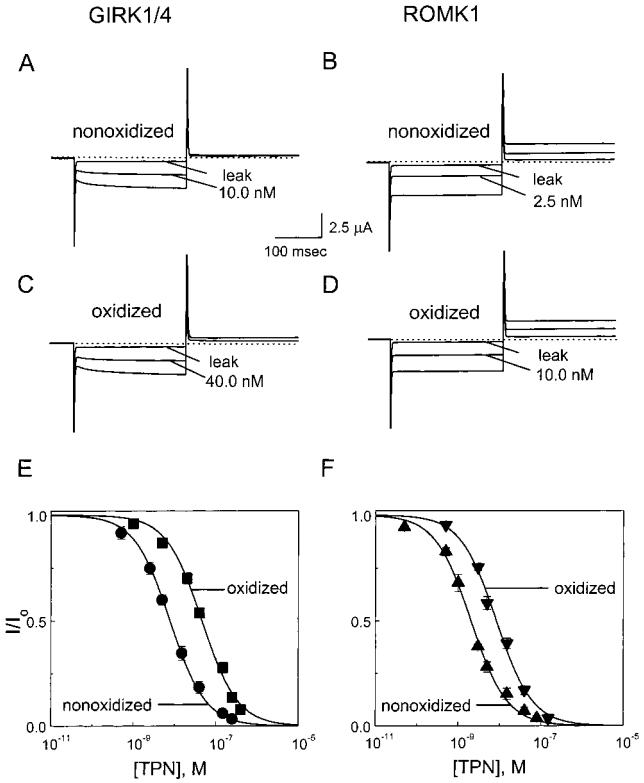

FIGURE 2: Oxidation of TPN hinders its interaction with both the GIRK1/4 and ROMK1 channels. A and B: Current traces of the GIRK1/4 and ROMK1 channels in the absence and presence of nonoxidized TPN, respectively. C and D: Current traces of the GIRK1/4 and ROMK1 channels in the absence and presence of oxidized TPN, respectively. The leak currents were recorded in the presence of TPN at concentrations greater than 100 times of the K_i values. The dashed lines identify the zero current level. E: The fractions of unblocked GIRK1/4 current (mean ± sem, $n = 3-26$) were plotted as a function of the concentrations of oxidized and nonoxidized TPN, respectively. F: The fractions of unblocked ROMK1 current (mean ± sem, $n = 4-50$) were plotted as a function of the concentration of oxidized and nonoxidized TPN, respectively. The curves superimposed on the data points in E and F correspond to the fits of equation $I/I_o = K_i/(K_i + [TPN])$. The fits yield that the K_i values for the GIRK1/4 channel to interact with nonoxidized and oxidized TPN are 8.3 ± 0.5 (mean ± sem) nM and 40.5 ± 0.7 nM, respectively, while those for the ROMK1 to interact with nonoxidized and oxidized TPN are 2.0 ± 0.2 nM and 7.8 ± 0.5 nM, respectively.

thermodynamic mutant cycle analysis (*47*, *60*, *61*). Previously, we found that a single alanine substitution for each of four P-region residues, N117, R118, F146, and F148, lowers the affinity of the ROMK1 channel for TPN by 10-fold or more (*57*). To identify the channel residue coupled to M13 in TPN, we examined the potential energetic coupling between M13 and each of the four channel residues with mutant cycle analysis. Figure 3 shows the four mutant cycles, in which the tested residues in both the channel and the toxin are mutated to alanine. For each channel−toxin pair, there are four possible combinations. One of the four combinations is shown at each corner of the mutant cycle box. X_{LF}, X_{RT}, Y_{UP}, and Y_{LW} are ratios of the corresponding adjacent K_i. The ratio of X_{LF} and X_{RT} (or Y_{UP} and Y_{LW}) defined as Ω can be used to evaluate the energetic coupling between two tested residues. All Ω values presented in the mutant cycle boxes are in a form greater than one, and their natural logarithm form is presented in Figure 4. Interestingly, when M13 in TPN was tested against channel residue F148, the mutant cycle analysis yielded an Ω value of 40. However, when it was tested against the other three channel residues, Ω values were ∼ 2. These results argue that M13 in TPN is energetically coupled to channel residue F148.

Table 1: K_i Values for TPN and Its Deriatives

	mean (nM)	sem	*n*
wt	2.04	0.02	50
M13A	19.31	2.51	4
M13D	21.54	1.82	4
M13E	299.63	17.65	4
M13F	33.74	1.98	3
M13G	96.81	6.32	4
M13I	7.21	0.45	8
M13L	16.23	1.91	4
M13N	40.41	3.04	4
M13Q	1.25	0.01	50
M13S	38.93	4.25	4
M13T	21.41	2.06	4
M13V	12.54	1.08	4
M13W	40.14	2.34	3
M13Y	27.12	1.65	3

A High Affinity and Stable TPN Derivative. Oxidation of M13 hinders the interaction of TPN with the channel. To overcome this problem, we substituted M13 with nonoxidizable residues, e.g., alanine. Although alanine substitution eliminates the oxidation problem, it introduces another problem—the derivative binds to the channel with a much lower affinity. To search for a TPN derivative with an affinity similar to the native one, we replaced M13, one at a time, by fourteen different residues (A, D, E, F, G, I, L, N, Q, S, T, V, W, and Y). Figure 5A shows current traces of the ROMK1 channels in the absence and presence of six representative TPN derivatives. For most TPN derivatives, much higher concentrations are needed to inhibit half of the current of the ROMK1 channel. Interestingly, one TPN derivative, M13Q (referred to as TPN_Q), binds to the ROMK1 channel with high affinity ($K_i = 1.3$ nM). The fractions of unblocked currents by those TPN derivatives are plotted against their concentrations in Figure 5B. We determined the K_i values of all TPN derivatives by fitting the inhibition data with an equation assuming that one TPN molecule blocks one channel (*62*). K_i values for all the fourteen TPN derivatives are summarized in Table 1.

Specificity Comparison between TPN and TPN_Q. We compared the specificity of TPN and TPN_Q among three inward-rectifier K^+ channels, GIRK1/4, ROMK1, and IRK1. Figure 6, A−C, shows the current traces of the three channels in the presence and absence of TPN, while Figure 6,D−F, shows those in the presence and absence of TPN_Q. TPN and TPN_Q at similar concentrations inhibited about half of the currents of the GIRK1/4 or the ROMK1 channel. However, the IRK1 channel is essentially insensitive to both TPN and TPN_Q at a concentration of 2 μM, consistent with our previous finding (*57*). The fraction of the unblocked currents for all three channels are plotted against the concentration of TPN and TPN_Q in Figure 6, G and H, respectively. The data show that TPN and TPN_Q have similar specificity among the three inward-rectifier K^+ channels.

DISCUSSION

The methionine residue in tertiapin becomes oxidized "spontaneously" and its oxidation affects the binding of TPN

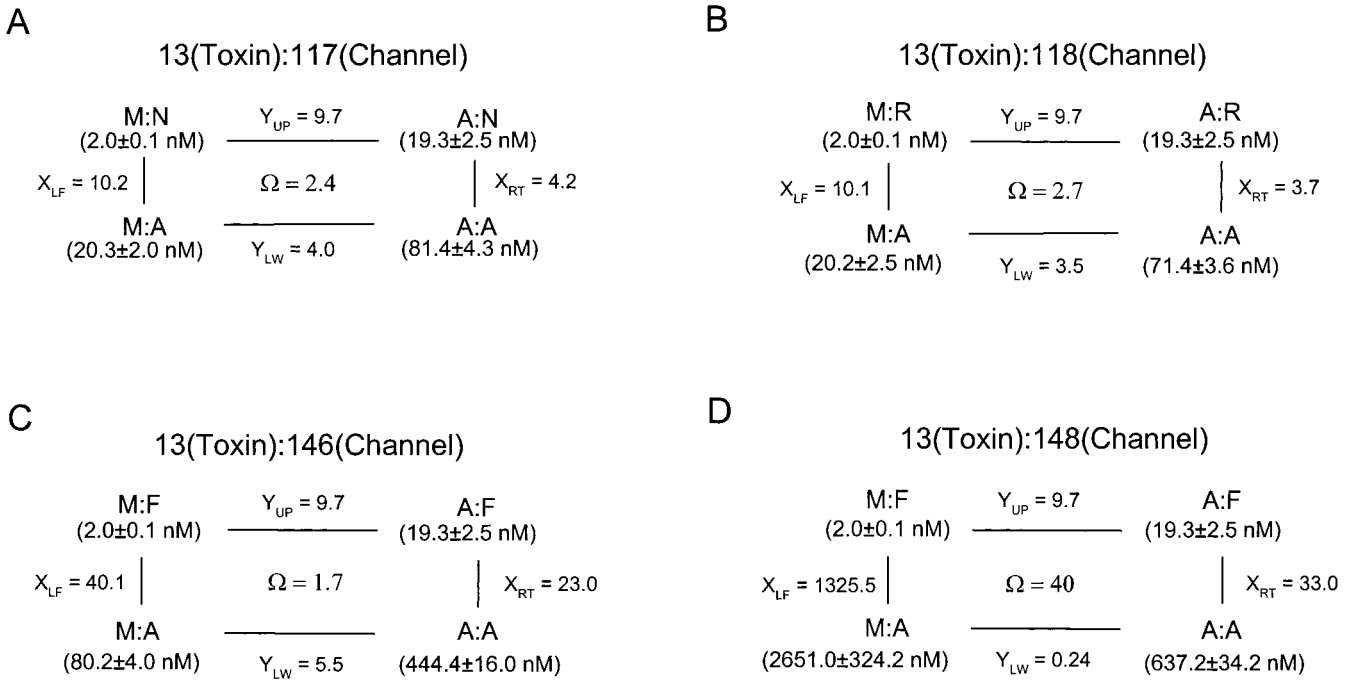

FIGURE 3: Thermodynamic mutant cycles. In each of the four mutant cycles, one channel residue is tested against residue 13 in TPN, as indicated above the mutant cycle boxes. Each of the four corners of a mutant cycle box represents a tested TPN−ROMK1 residue pair in single letter codes. The four corners are wild-type TPN vs wild-type ROMK1 (upper left), wild-type TPN vs mutant ROMK1 (lower left), mutant TPN vs wild-type ROMK1 (upper right) and mutant TPN vs mutant ROMK1 (lower right). In each case, the tested residue was replaced by alanine. The K_i values (mean ± sem) for each tested pair is presented in the corresponding parentheses. X and Y are the ratios of the adjacent K_i values. The Ω values are the ratios of X_{LF} and X_{RT} (or Y_{UP} and Y_{LW}).

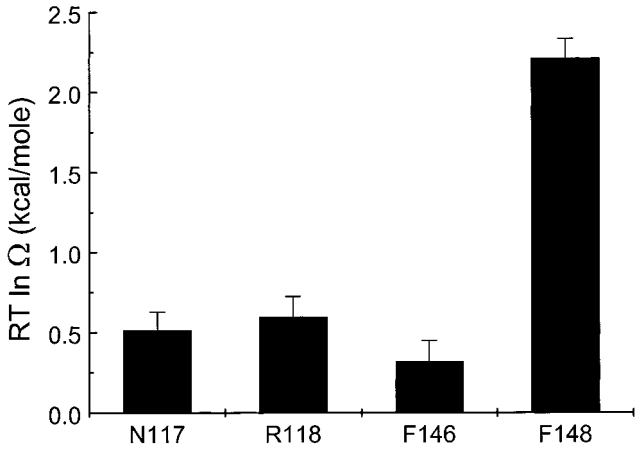

FIGURE 4: Values of RT ln Ω (mean ± sem) associated with the four ROMK1 residues when tested against M13 in TPN.

to the targeted channels. In fact, many scorpion toxins inhibiting voltage- and Ca^{2+}-activated K^+ channels also contain methionine residues. In some cases, methionine residues in those toxins are critical for the channel-toxin interaction (*43*, *44*, *48*−*50*). However, there has been no documented information thus far on either oxidizability of the methionine residues in those scorpion toxins by air or any resulting alteration in the channel-toxin interaction.

Generally, the sulfur atom in the side-chain of methionine is susceptible to oxidation by air or other oxidants. A complete oxidation of the sulfur atom in a methionine residue is a two-step reaction. In the first step, sulfoxide is formed by covalently attaching a single oxygen atom to the sulfur. This step of the reaction can be reversed by thiols (*63*). However, formation of sulfone in the second step by covalently attaching a second oxygen atom to sulfoxide is irreversible. We only observed the first oxidation step with TPN. The formation of sulfoxide in TPN significantly hinders its binding to both the GIRK1/4 and the ROMK1 channels (Figure 2). Although the oxidation of the methionine residue can be reversed with a reducing agent, the amount of reducing agent needed also reduces the disulfide bonds within TPN, thereby rendering it nonfunctional.

Oxidation of TPN significantly limits its applicability. To overcome this problem we replaced M13 with fourteen different residues. Out of them, only the derivative containing a glutamine residue at position 13, TPN_Q, binds to the ROMK1 channel with a high affinity similar to that of native TPN (Table 1). Like TPN, TPN_Q also blocks the GIRK1/4 channel with high affinity but does not inhibit the IRK1 channel, and thus has the same specificity among the three inward-rectifier K^+ channels (Figure 6). We do not have a definitive explanation why a glutamine residue provides a nearly full energetic compensation for the methionine in TPN. However, it is interesting to note that the accessible surface areas of the side-chain of glutamine (and phenylalanine) are closest to that of methionine among all naturally existing neutral amino acids, but the ratios of polar and nonpolar portions are very different between the two (*64*). Furthermore, among those neutral residues only the side-chains of methionine (C−C−S−C) and glutamine (C−C−C−N(or O)) have four linear non-hydrogen atoms.

To identify the channel residue that is energetically coupled to M13 in TPN, we carried out thermodynamic mutant cycle analysis. The theoretical basis of the analysis has been thoroughly discussed in many earlier papers by other investigators (*47*−*50*, *60*, *61*). Here, we just recapture its essence. If a channel residue is not coupled to a toxin residue (i.e., they are independent), then the binding energy

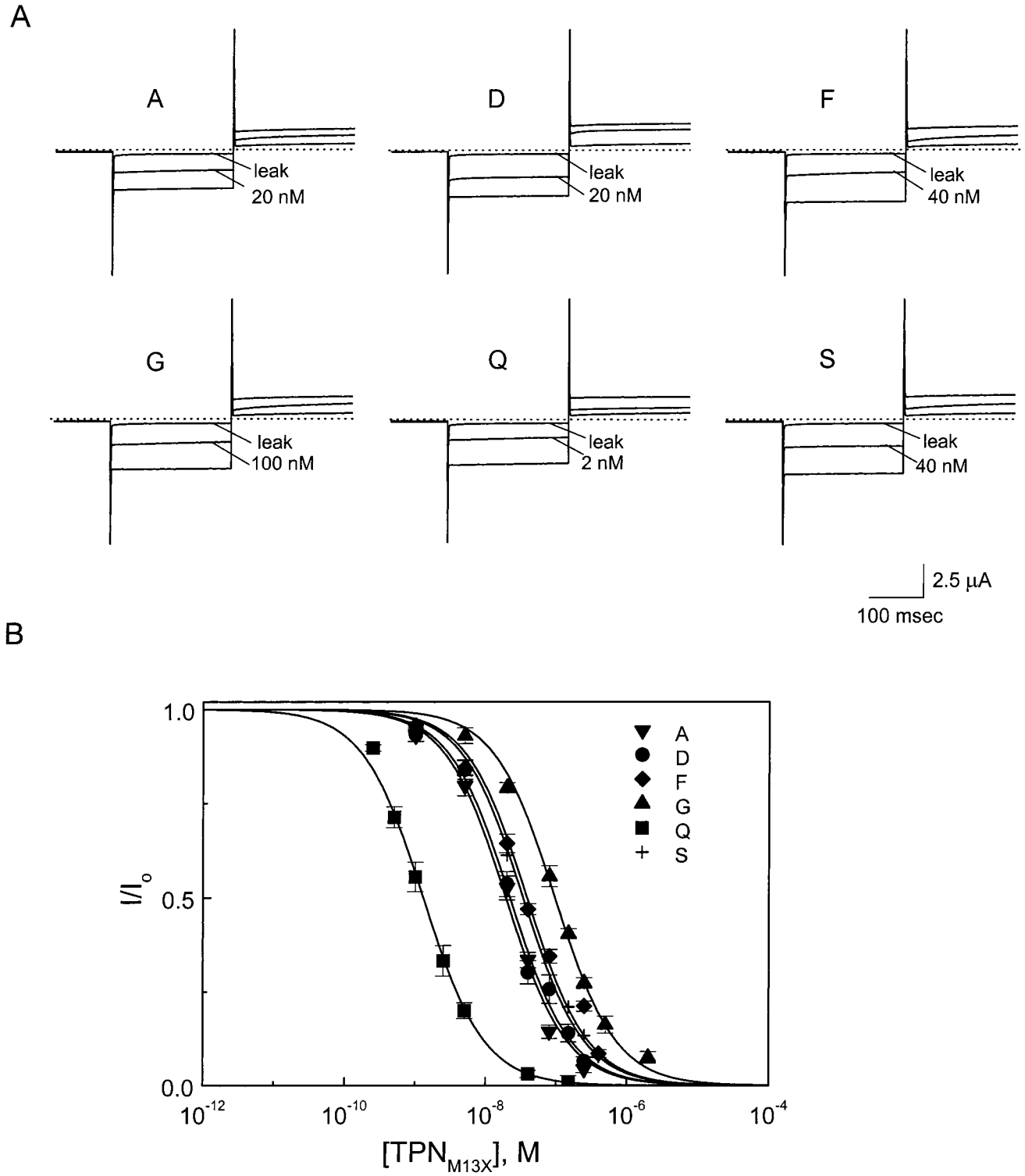

FIGURE 5: Effects of M13 mutations on the interaction of TPN with the channel. A: Current traces of the ROMK1 channel in the absence and presence of six representative TPN derivatives in which M13 was replaced by the residue indicated. B: The fractions of unblocked currents (mean ± sem, $n = 4-50$) were plotted as a function of the concentration of TPN derivatives. The curves superimposed on the data points correspond to the fits of equation $I/I_o = K_i/(K_i + [TX])$.

changes due to mutating both the channel and toxin residues should be additive. Consequently, the difference in free energy changes that results from mutating one tested residue with and without mutating the other tested residue ($RT\ln \Omega$) should theoretically be zero. Conversely, if the value of $RT\ln \Omega$ deviates significantly from zero, an energetic coupling between the tested channel and the toxin residues is indicated, provided the large value of Ω is unique. Generally, a unique large Ω value argues against a global structural change caused by the mutation, because energy changes caused by a global structural change would be distributed over many residues at the interface, which would result in large Ω values when a toxin residue is tested against many channel residues.

As shown in Figure 4, when M13 in TPN is tested against channel residue F148 the value of $RT\ln \Omega$ is 2.2 kcal/mol,

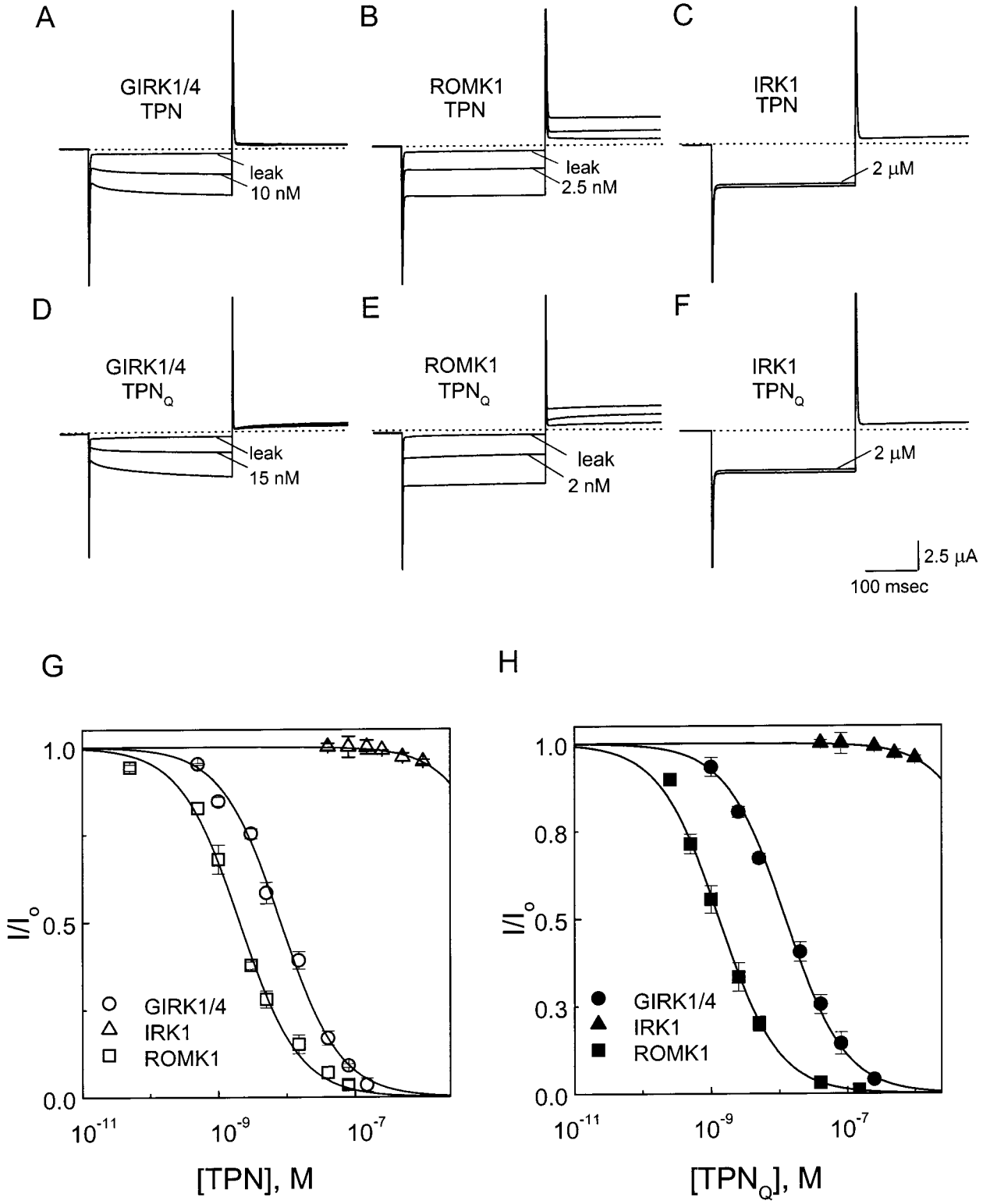

FIGURE 6: Comparison of specificity of TPN and TPN_Q among three inward-rectifier K^+ channels. A−C: Current traces of GIRK1/4, ROMK1, and IRK1 in the absence and presence of TPN at the concentrations indicated. D−F: Current traces of GIRK1/4, ROMK1, and IRK1 in the absence and presence of TPN_Q at the concentrations indicated. The leak currents were obtained in the presence of TPN_Q at concentrations greater than 100 times of the corresponding K_i values, except for the IRK1 channel whose affinities for TPN and TPN_Q are too low. The dashed lines identify the zero current level. G: The fractions of unblocked currents of the GIRK1/4, ROMK1, and IRK1 channels were plotted as a function of the concentration of TPN. H: The fractions of unblocked currents of the GIRK1/4, ROMK1, and IRK1 channels were plotted as a function of the concentration of TPN_Q. All data in G and H were corrected for background leak currents, except for those of IRK1. The curves superimposed on the GIRK1/4 and ROMK1 data points in G and H correspond to the fits of equation $I/I_o = K_i/(K_i + [TX])$. The K_i values determined from the fits are 8.3 ± 0.5 nM (mean ± sem), 2.0 ± 0.2 nM, 13.3 ± 0.6 nM, and 1.3 ± 0.1 nM for GIRK1/4-TPN, ROMK1-TPN, GIRK1/4-TPN_Q, and ROMK1-TPN_Q interactions, respectively. The curves superimposed on the IRK1 data points have no theoretical significance.

whereas those values associated with the other three channel residues, when tested against residue 13 in the toxin, are about 0.5 kcal/mol or less. These results argue that residue 13 in the toxin is coupled to residue 148 in the channel. This

interpretation of our results is compatible with the observation made in the study correlating the values of $RT\ln \Omega$ (referred there as $\Delta\Delta G$) with the distances between the residues at the interface of a protein−protein (barnase-barstar) complex of known structure. That study showed that a value of $RT\ln \Omega$ greater than 1 kcal/mol generally associates with one barnase residue and one barstar residue less than 4 Å apart, the expected distance range between the residues interacting directly with each other (*61*).

Furthermore, we also tested Q13 in TPN_Q against F148 in ROMK1, which yielded a $RT\ln \Omega$ value of 1.5 ± 0.1 kcal/mol. This finding shows that residue 13 in TPN is energetically coupled to residue148 in ROMK1, regardless of whether a methionine or glutamine residue is present at position 13. Thus, the glutamine mutation in TPN does not appear to cause a significant change in the overall structure of TPN.

According to the structural model of the bacterial KcsA channel based on crystallographic studies, residue F148 in the ROMK1 channel would be located at the base of the external vestibule, just outside of the narrowest region of the K^+ pore (*9*). TPN consists of an α-helix formed by residues 12−19 and a type-I reverse turn formed by residues 4−7 connected by a loop (*65*). M13 in TPN is located at the N-terminal end of the α-helix. Thus, a coupling between channel residue F148 and TPN residue M13 suggests that the α-helix may form the interaction surface in TPN, which would be different from that in scorpion toxins where the interaction surface is formed primarily by the β-strands (*43*, *44*, *49*).

In summary, we reported, here, that oxidation of methionine 13 in TPN hinders its binding to the targeted channels. To circumvent this problem, we synthesized a TPN derivative with a glutamine residue at position 13. The synthesized TPN_Q is stable and functionally resembles native TPN, and, therefore, will be a very useful molecular probe for studying the inward-rectifier K^+ channels.

ACKNOWLEDGMENT

We thank D.E. Clapham for the CIR clone, K. Ho and S. Hebert for the ROMK1 clone, L.Y. Jan for GIRK1 and IRK1 clones, and E.G. Peralta for HM2 and HM4 clones. We also thank C. Deutsch for critical reading of our manuscript, A. M. Klem for manuscript preparation and technical assistance, and J. Rush for a helpful discussion. Mass spectrometry and peptide synthesis were performed by the Biopolymer Facility, Harvard Medical School.

REFERENCES

1. Hille, B. (1991) *Ionic channels of excitable membranes*, Sinauer Associates, Inc., Sunderland, MA.
2. Ho, K., Nichols, C. G., Lederer, W. J., Lytton, J., Vassilev, P. M., Kanazirska, M. V., and Hebert, S. C. (1993) *Nature 362*, 127−132.
3. Kubo, Y., Baldwin, T. J., Jan, Y. N., and Jan, L. Y. (1993) *Nature 362*, 127−132.
4. Kubo, Y., Reuveny, E., Slesinger, P. A., Jan, Y. N., and Jan, L. Y. (1993) *Nature 364*, 802−806.
5. Dascal, N., Schreibmayer, W., Lim, N. F., Wang, W., Chavkin, C., DiMagno, L., Labarca, C., Kieffer, B. L., Gaveriaux-Ruff, C., Trollinger, D., Lester, H., and Davidson, N. (1993) *Proc. Natl. Acad. Sci. U.S.A.* 90, 10235−10239.
6. Krapivinsky, G., Gordon, E. A., Wickman, K., Velimirovic, B., Krapivinsky, L., and Clapham, D. E. (1995) *Nature 374*, 135−141.
7. Inagaki, N., Gonoi, T., Clement, J. P., IV, Namba, N., Inazawa, J., Gonzalez, G., Aguilar-Bryan, L., Seino, S., and Bryan, J. (1995) *Science 270*, 1166−1170.
8. Heginbotham, L., Lu, Z., Abramson, T., and MacKinnon, R. (1994) *Biophys. J. 66*1061−1067.
9. Doyle, D., Cabral, J. M., Pfuetzner, R. A., Kuo, A., Gulbis, J. M., Cohen, S. L., Chait, B. T., and MacKinnon, R. (1998) *Science 280*, 69−77.
10. Miller, C., Modzydlowski, E., Latorre, R., and Phillips, M. (1985) *Nature 331*, 316−318.
11. Gimenez-Gallego, G., Navia, M. A., Reuben, J. P., Katz, G. M., Kaczorowski, G. J., and Garcia, M. L. (1988) *Proc. Natl. Acad. Sci. U.S.A.* 85, 3329−3333.
12. Haux, P., Sawerthal, H., and Habermann, E. (1967) *Physiol. Chem. 348*, 737−738.
13. Shipolini, R. A., Bradbury, A. F., Callewaet, G. L., and Vernon, C. A. (1967) *Chem. Commun. 1*, 679−680.
14. Billingham, E. E. J., Morley, J., Hanson, J. M., Shipolini, R. A., and Vernon, C. A. (1973) *Nature 245*, 163−164.
15. Harvey, A. L., and Karlsson, E. (1980) *Naunyn−Schmiedeberg's Arch. Pharmacol. 312*, 1−6.
16. Possani, L. D., Martin, B. M., and Svendsen, I. B. (1982) *Carlsberg Res. Commun. 47*, 285−289.
17. Halliwell, J. V., Othman, I. B., Pelchen-Matthews, A., and Dolly, J. O. (1986). *Proc. Natl. Acad. Sci. U.S.A.* 83, 942−944.
18. Penner, R., Petersen, M., Pierau, F.-K., and Dreyer, F. (1986) *Pflügers Arch. 407*, 365−369.
19. Smith, C., Phillips, M., and Miller, C. (1986) *J. Biol. Chem. 261*, 14607−14613.
20. Stansfeld, C. E., Marsh, S. J., Halliwell, J. V., and Brown, D. A. (1986) *Neurosci. Lett. 64*, 299−304.
21. Carbone, E., Prestipino, G., Spadavecchia, L., Franciolini, F., and Possani, L. D. (1987) *Pflügers Arch. 408*, 423−431.
22. Chicchi, G. G., Gimenez-Gallego, G., Ber, E., Garcia, M. L., Winquist, R., and Cascieri, M. A. (1988) *J. Biol. Chem. 263*, 10192−10197.
23. Lucchesi, K., Ravindran, A., Young, H., Moczydlowski, E. (1989) *J. Membr. Biol. 109*, 269−281.
24. Galvez, A., Gimenez-Gallego, G., Reuben, J. P., Roy-Contancin, L., Feigenbaum, P., Kaczorowski, G. J., and Garcia, M. L. (1990) *J. Biol. Chem. 265*, 11083−11090.
25. Crest, M., Jacquet, G., Gola, M., Zerrouk, H., Benslimane, A., Rochat, H., Mansuelle, P., and Martin-Eauclaire, M.-F. (1992) *J. Biol. Chem. 267*, 1640−1647.
26. Garcia-Calvo, M., Leonard, R. J., Novick, J., Stevens, S. P., Schmalhofer, W., Kaczorowski, G. J., and Garcia, M. L. (1993) *J. Biol. Chem. 268*, 18866−18874.
27. Werkman, T. R., Gustafson, T. A., Rogowski, R. S., Blaustein, M. P., and Rogawski, M. A. (1993) *Mol. Pharmacol.* 44, 430−436.
28. Garcia, M. L., Garcia-Calvo, M., Hidalgo, P., Lee, A. W., and MacKinnon, R. (1994) *Biochemistry 33*, 6834−6839.
29. Swartz, K. J., and MacKinnon, R. (1995) *Neuron 15*, 941−949.
30. Blatz, A. L., and Magleby, K. L. (1986) *Nature 323*, 718−720.
31. Stuhmer, W., Ruppersburg, J. P., Schroter, K. H., Sakmann, B., Stocker, M., Giese, K. P., Perschke, A., Baumann, A., and Pongs, O. (1989) *EMBO J. 8*, 3235−3244.
32. Stansfeld, C. E., Marsh, J. J., Parcej, D. N., Dolly, D. O., and Brown, D. A. (1987) *Neuroscience 23*, 893−902.
33. Brau, M. E., Dreyer, F., Jonas, P., Repp, H., and Vogel, W. (1990) *J. Physiol. 420*, 365−385.
34. Benishin, C. G., Sorensen, R. G., Brown, W. E., Krueger, B. K., and Blaustein, M. P. (1988) *Mol. Pharmacol. 34*, 152−159.
35. Muniz, Z. M., Diniz, C. R., and Dolly, J. O. (1990) *J. Neurochem. 54*, 343−346.
36. Kirsh, G. E., Drewe, J. A., Verma, S., Brown, A. M., and Joho, R. H. (1991) *FEBS Lett. 278*, 55−60.

37. Harvey, A. L., and Anderson, A. J. (1991) in *Snake Venoms* (Harvey, A. L., Ed.) pp 131−164, Pergamon Press.
38. MacKinnon, R., and Miller, C. (1988) *J. Gen. Physiol. 91*, 335−349.
39. Miller, C. (1988) *Neuron 1*, 1003−1006.
40. Park, C.-S., and Miller, C. (1992) *Neuron 9*, 307−313.
41. MacKinnon, R., and Miller, C. (1989). *Science 245*, 1382−1385.
42. MacKinnon, R., Heginbotham, L., and Abramson, T. (1990) *Neuron 5*, 767−771.
43. Stampe, P., Kolmakova-Partensky, L., and Miller, C. (1994) *Biochemistry 31*, 443−450.
44. Goldstein, S. A. N., Pheasant, D. J., and Miller, C. (1994) *Neuron 12*, 1377−1388.
45. Stocker, M., and Miller, C. (1994) *Proc. Natl. Acad. Sci. U.S.A. 91*, 9509−9513.
46. Gross, A., Abramson, T., and MacKinnon, R. (1994) *Neuron 13*, 961−966.
47. Hidalgo, P., and MacKinnon, R. (1995) *Science 268*, 307−310.
48. Aiyar, J., Withka, J. M., Rizzi, J. P., Singleton, D. H., Andrews, G. C., Lin, W., Boyd, J., Hanson, D. C., Simon, M., Dethlets, B., Lee, C. L., Hall, J. E., Gutman, G. A., and Chandy, K. G. (1995) *Neuron 15*, 1169−1181.
49. Rangananthan, R., Lewis, J. H., and MacKinnon, R. (1996) *Neuron 16*, 131−139.
50. Naranjo, D., and Miller, C. (1996) *Neuron 16*, 123−130.
51. Gross, A., and MacKinnnon, R. (1996) *Neuron 16*, 399−406.
52. MacKinnon, R., Cohen, S. L., Kuo, A., Lee, A., and Chait, B. T. (1998) *Science 280*, 106−109.
53. Swartz, K. J., and MacKinnon, R. (1997) *Neuron 18*, 665−673.
54. Swartz, K. J., and MacKinnon, R. (1997) *Neuron 18*, 675−682.
55. Lu, Z., and MacKinnon, R. (1997) *Biochemistry 36*, 6936−6940.
56. Imredy, J., Chen, C., and MacKinnon, R. (1998) *Biochemistry 37*, 14867−14874.
57. Jin, W., and Lu, Z. (1998) *Biochemistry 38*, 13291−13299.
58. Gauldie, J., Hanson, J. M., Rumjanek, F. D., Shipolini, R. A., and Vernon, C. A. (1976) *Eur. Biochem. 61*, 369−376.
59. Ovchinnikov, Y. A., Miroshnikov, A. I., Kudelin, A. B., Kostina, M. B., Boikov, V. A., Magzanik, L. G., and Gotgilf, I. M. (1980) *Bioorg. Khim. 6*, 359−365.
60. Horovitz, A., and Fersht, A. R. (1990) *J. Mol. Biol. 214*, 613−617.
61. Schreiber, G., and Fersht, A. R. (1995) *J. Mol. Biol. 248*, 478−486.
62. Jin, W., Klem, A. M., Lewis, J. H., and Lu, Z. (1999) *Biochemistry 37*, 14294−14301.
63. Creighton, T. E. (1993) *Proteins: structures and molecular properties*, W. H. Freeman and Company. New York.
64. Miller, S., Janin, J., Lesk, A. M., and Chothia, C. (1987) *J. Mol. Biol. 196*, 641−656.
65. Xu, X., and Nelson, J. W. (1993) *Protein: Struct. Funct., Genet. 17*,124−137.

BI991205R